

REPORT

OPEN ACCESS



A bivalent, bispecific Dab-Fc antibody molecule for dual targeting of HER2 and HER3

Alexander Rau ^a, Katharina Kocher ^a, Mirjam Rommel ^a, Lennart Kühl ^a, Maximilian Albrecht ^a,
Hannes Gotthard ^a, Nadine Aschmoneit ^a, Bettina Noll^a, Monilola A. Olayioye ^{a,b}, Roland E. Kontermann ^{a,b},
and Oliver Seifert ^{a,b}

^aInstitute of Cell Biology and Immunology, University of Stuttgart, Stuttgart, Germany; ^bStuttgart Research Center Systems Biology (SRCSB), University of Stuttgart, Stuttgart, Germany

ABSTRACT

Dual targeting of surface receptors with bispecific antibodies is attracting increasing interest in cancer therapy. Here, we present a novel bivalent and bispecific antagonistic molecule (Dab-Fc) targeting human epidermal growth factors 2 and 3 (HER2 and HER3) derived from the Db-Ig platform, which was developed for the generation of multivalent and multispecific antibody molecules. Dab-Fc comprises the variable domains of the anti-HER2 antibody trastuzumab and the anti-HER3 antibody 3–43 assembled into a diabody-like structure stabilized by C_H1 and C_L domains and further fused to a human γ 1 Fc region. The resulting Dab-Fc 2 \times 3 molecule retained unhindered binding to both antigens and was able to bind both antigens sequentially. In cellular experiments, the Dab-Fc 2 \times 3 molecule strongly bound to different tumor cell lines expressing HER2 and HER3 and was efficiently internalized. This was associated with potent inhibition of the proliferation and migration of these tumor cell lines. Furthermore, IgG-like pharmacokinetics and anti-tumoral activity were demonstrated in a xenograft tumor model of the gastric cancer cell-line NCI-N87. These results illustrate the suitability of our versatile Db-Ig platform technology for the generation of bivalent bispecific molecules, which has been successfully used here for the dual targeting of HER2 and HER3.

ARTICLE HISTORY

Received 20 October 2020
Revised 22 February 2021
Accepted 8 March 2021

KEYWORDS

Bispecific antibody; diabody-ig; Db-Ig; dual targeting; HER2; HER3

Introduction

The human epidermal growth factor receptor family member HER2 (ErbB2) is an established target structure in cancer therapy.¹ HER2 is highly overexpressed in ~20% of primary invasive breast cancers, and HER2 aberrations were also identified in gastric cancer, as well as biliary tract, colorectal, non-small-cell lung and bladder cancers.^{2–4} Activation of the epidermal growth factor receptor (EGFR) family members by dimerization can lead to several cellular responses involved in tumor formation and progression. While EGFR, HER3 and HER4 require ligand-mediated conformational changes for dimerization with members of the EGFR family and subsequent activation of downstream signals, HER2 is locked in an open conformation and is thus a preferred dimerization partner for the other HER family members.⁵ HER2 can also form homodimers, especially when overexpressed by tumor cells. Two HER2-specific monoclonal antibodies (trastuzumab and pertuzumab), inhibiting receptor dimerization and activation, are approved for the treatment of HER2-overexpressing metastatic breast and gastric cancers.⁶ Furthermore, pan-specific small-molecule inhibitors of the kinase domains, such as lapatinib and afatinib, are approved to treat HER2-dependent tumors.⁶ Although these molecules have strongly improved the therapeutic responses, resistance to HER2-targeting therapies eventually

evolves in many patients.⁷ Compensatory activation of the heregulin (HRG)/HER3 pathway through upregulation of HER3 or release of the HER3 ligand (HRG) by the surrounding tumor stroma has been shown to contribute to treatment failure and poor outcome in several tumor entities.^{6,8–10} HER3 is the preferred heterodimerization partner of HER2 and efficiently activates the PI3K/Akt growth and survival pathway.^{11–13} HER3 has, therefore, been recognized as an important driver of resistance to HER2 therapy.¹⁴

We have recently generated a novel HER3 antibody, IgG 3–43, which efficiently blocks ligand-dependent and the -independent receptor activation and inhibited tumor cell growth in vitro and in vivo.¹⁵ In a further study, this antibody was combined with a humanized version of cetuximab into a tetravalent bispecific scDb-Fc fusion protein targeting EGFR and HER3. In triple-negative breast cancer cell lines (TNBC), we showed that treatment with a bispecific antibody inhibited not only general proliferation but also the survival and expansion of the cancer stem cell population.¹⁶

Dual targeting of HER2 and HER3 has emerged as a novel treatment option to overcome the limitations of HER2 targeting.^{17–19} This can be achieved, for example, by combining antibodies against HER2 and HER3, or by using bispecific antibodies.^{20–23} A plethora of bispecific antibody formats have been developed in the past decades, and several formats

have been evaluated for dual targeting of members of the EGFR family.²⁴ However, in vitro studies with tetravalent bispecific antibodies targeting HER2 and HER3, i.e., exhibiting two binding sites for each antigen, revealed agonistic activity as shown, for example, for an IgG-single-chain variable fragment (scFv) fusion protein.²⁰ This finding is in line with our own initial studies on a tetravalent bispecific antibody directed against HER2 and HER3 using the same scDb-Fc format successfully applied for dual targeting of EGFR and HER3.¹⁶ There is evidence that this agonistic activity, presumably resulting from receptor cross-linking, might be circumvented by using bivalent bispecific antibody formats.^{21,22}

Here, we have developed a bivalent, bispecific antibody targeting HER2 and HER3 by combining the antigen-binding site of IgG 3–43 with that of the HER2-neutralizing antibody trastuzumab, using our recently established Db-Ig platform technology.²⁵ In this novel format, a C_H1/C_L-stabilized bivalent and bispecific diabody is fused to a heterodimerizing Fc region. This Dab-Fc 2 × 3 molecule retained antigen-binding activity and efficiently inhibited HRG-mediated receptor activation. Furthermore, it reduced tumor cell proliferation and migration more efficiently than the parental antibodies, applied individually or in combination. Anti-tumor activity was demonstrated in a xenograft tumor model with the gastric cancer cell-line NCI-N87 subcutaneously transplanted into severe combined immunodeficiency (SCID-beige) mice. Importantly, we could demonstrate that the novel bivalent bispecific antibody targeting HER2 and HER3 lacks agonistic activity and exhibits IgG-like pharmacokinetic properties, making it a suitable candidate for further therapeutic developments.

Results

A bivalent bispecific Dab-Fc targeting HER2 and HER3

Initially, a tetravalent bispecific antibody targeting HER2 and HER3 was generated using a scDb-Fc format as used in a previous study.¹⁶ In this bispecific antibody, we combined the antigen-binding sites of trastuzumab and antibody 3–43. The antibody was successfully produced, purified and showed binding to both antigens in an enzyme-linked immunosorbent assay (ELISA) and to the breast cancer cell-line MCF-7 (Fig. S1). In vitro studies revealed, however, an agonistic activity for HER2 resulting in increased pHER2 and pERK levels, e.g., shown for MCF-7 cells. In contrast, the bivalent bispecific scDb moiety itself was also produced efficiently, and it was devoid of agonistic activity (Fig. S2). However, scDb molecules with a molecular mass of ~50 kDa suffer from a short serum half-life and lack Fc-mediated effector function. This motivated us to generate a bivalent bispecific antibody derivative directed against HER2 and HER3 that included an Fc region for extended half-life.²⁶

We used our Db-Ig technology, to generate a bivalent bispecific antibody composed of a C_H1/C_L-stabilized diabody (Dab) fused to an Fc region.²⁵ In this Dab-Fc format, the V_HA-V_LB domains are fused to a human γ 1 C_H1-C_H2-C_H3_{hole} chain and the V_HB-V_LA domains are fused to a complementary human γ 1 C_L-C_H2-C_H3_{knob} chain, respectively, resulting in a heterodimeric molecule (Figure 1a). This Dab-Fc 2 × 3 molecule was produced in transiently transfected HEK293-6E cells and purified by protein G affinity chromatography followed by a preparative size-exclusion chromatography (SEC) step. The SDS-PAGE analysis of the purified protein showed a single

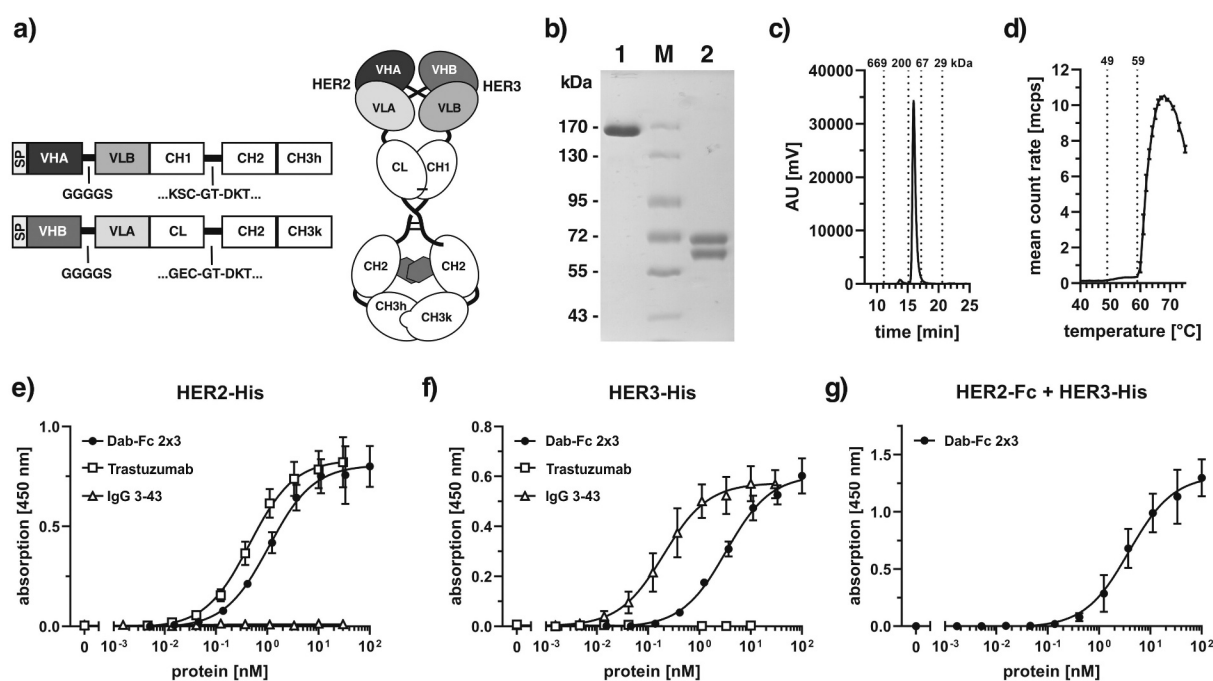


Figure 1. A bivalent bispecific Dab-Fc antibody targeting HER2 and HER3. a) Schematic structure of a Dab-Fc fusion protein. b) SDS-PAGE of anti-HER2xHER3 Dab-Fc (Dab-Fc 2 × 3) under non-reducing (1) and reducing (2) conditions. Four micrograms of protein was loaded per lane, M = Marker. c) size-exclusion chromatography of purified Dab-Fc 2 × 3. d) determining melting points (T_m) by dynamic light scattering. e) binding of Dab-Fc 2 × 3 to immobilized HER2-His in ELISA. f) binding of Dab-Fc 2 × 3 to immobilized HER3-His in ELISA. Trastuzumab and IgG 3–43 were included as controls. g) Sandwich ELISA testing binding of HER3-His to titrated Dab-Fc 2 × 3 bound to immobilized HER2-Fc. Mean ± SD, n = 3.

Table 1. EC₅₀ values [nM] of parental antibodies and bispecific Dab-Fc 2 × 3 molecule determined by ELISA-binding analysis.

	HER2-His [nM]	HER3-His [nM]	HER2-Fc + HER3-His [nM]
Trastuzumab	0.45 ± 0.02	n.d.	-
IgG 3-43	n.d.	0.21 ± 0.07	-
Dab-Fc 2x3	1.1 ± 0.1	3.3 ± 0.4	4.1 ± 1.2

The bispecific and bivalent Dab-Fc 2 × 3 was titrated in the bifunctional binding of HER2 and HER3. n.d.: not determined; -: not performed; Mean ± SD, n = 3.

band under non-reducing conditions with an apparent molecular mass of ~160 kDa, and under reducing conditions two bands with apparent molecular masses of 60 and 70 kDa, corresponding approximately to the calculated molecular masses of 61 and 63 kDa for the non-glycosylated polypeptides (Figure 1b). In analytical SEC, Dab-Fc 2 × 3 eluted with a major peak with an apparent molecular mass of ~120 kDa (Figure 1c). Dynamic light scattering revealed a first melting temperature (T_m) of 49°C and a second, major T_m of 59°C (Figure 1d).

Antigen-binding activity was confirmed by ELISA (Figure 1e, f). Here, Dab-Fc 2 × 3 showed binding to the immobilized extracellular regions of HER2 (HER2-His) and HER3 (HER3-His), with EC₅₀ values of 1.1 nM and 3.3 nM, respectively. In contrast, trastuzumab specifically bound only to HER2-His (EC₅₀ value 0.45 nM), while the anti-HER3 antibody IgG 3-43 bound specifically to HER3-His (EC₅₀ value 0.21 nM). The increased binding of the bivalent IgG molecules is presumably due to avidity effects, not seen for the Dab-Fc, which binds monovalently to each antigen. Sequential binding to both antigens of Dab-Fc 2 × 3 was further confirmed by a sandwich-ELISA with immobilized HER2-Fc incubated with a titration of Dab-Fc 2 × 3 followed by incubation with HER3-His (Figure 1g). Thus, Dab-Fc 2 × 3 retained antigen-binding specificity and the ability to bind to both antigens sequentially (Table 1).

Cell binding, internalization and antibody-dependent cell-mediated cytotoxicity

Cell binding of Dab-Fc 2 × 3 was analyzed with a panel of tumor cell lines expressing different HER2 and HER3 receptor levels on their surfaces. Data for three breast cancer cell lines, MCF-7 (~21,000 HER2/cell, ~17,000 HER3/cell), BT474 (>570,000 HER2/cell, ~11,000 HER3/cell), and SKBR3 (>570,000 HER2/cell, ~14,000 HER3/cell), and one gastric cancer cell-line NCI-N87 (>570,000 HER2/cell, ~3,300 HER3/cell), confirmed concentration-dependent binding of Dab-Fc 2 × 3 and the parental antibodies, with EC₅₀ values between 3.3 nM and 7.4 nM. Strong binding was seen for trastuzumab on all four cell lines, especially BT474, SKBR3, and NCI-N87, expressing high numbers of HER2. Due to the low expression levels of HER3, IgG 3-43 showed weak binding to these three cell lines while binding to MCF-7 cells, expressing approximately equal numbers of HER2 and HER3 was in the picomolar range (EC₅₀ value 15 pM). Dab-Fc showed strong binding to all four cell lines. Compared to trastuzumab, the binding of Dab-Fc 2 × 3 was ~3- to sixfold weaker, presumably due to monovalent binding to HER2 and HER3 (Table 2). All experiments were performed on the gastric cancer cell-line NCI-N87

Table 2. EC₅₀ values [nM] of parental antibodies and bispecific Dab-Fc 2 × 3 molecule determined by flow cytometry analysis.

	MCF-7 [nM]	BT474 [nM]	SKBR3 [nM]	NCI-N87 [nM]
Trastuzumab	0.7 ± 0.6	1.3 ± 0.4	1.7 ± 0.6	1.2 ± 0.7
IgG 3-43	0.015 ± 0.004	0.012 ± 0.007	0.013 ± 0.001	0.009 ± 0.002
Dab-Fc 2x3	4.1 ± 1.8	4.6 ± 1.5	7.4 ± 4.9	3.3 ± 1.8

Mean ± SD, n = 3.

and additionally tested on cells originating from the breast cancer system.

Binding of the bispecific antibodies to HER2 and HER3 might trigger receptor-mediated internalization and subsequent receptor degradation, with possible applications for intracellular delivery of the antibody. The internalization of Dab-Fc 2 × 3 in comparison to trastuzumab and IgG 3-43 was studied with pHrodo-labeled proteins. Labeling of proteins only slightly reduced binding (~2-fold) to HER2 and/or HER3 in ELISA (not shown). Incubating NCI-N87 cells for up to 48 hours at 37°C with the labeled Dab-Fc 2 × 3 resulted in strong internalization of the bispecific antibody, similar to trastuzumab, while IgG 3-43 showed weaker signals due to the lower HER3 levels on NCI-N87 (Figure 2e, f). Additionally, internalization was analyzed on MCF-7 cells expressing similar amount of HER2 and HER3 on the cell surface. In this experiment, IgG 3-43 showed high internalization in accordance with strong binding of this antibody, followed by the internalization of Dab-Fc and trastuzumab (Fig. S3). In contrast, incubation at 4°C resulted in only a small increase in signal during the first 6 hours, which then declined during the incubation period. Thus, Dab-Fc 2 × 3 is efficiently internalized into HER2/HER3 expressing cells at physiological temperature. Additionally, after 6 and 24 hours, we observed reduced amounts of HER3 in the cells treated with either the bispecific Dab-Fc 2 × 3 or with IgG 3-43 (alone or in combination) compared to those in non-treated or trastuzumab-treated cells (Fig. S4).

Furthermore, using NCI-N87 cells and human peripheral blood mononuclear cells (PBMCs), we found that the bispecific Dab-Fc 2 × 3 antibody and trastuzumab induced antibody-dependent cell-mediated cytotoxicity (ADCC) to a similar extent. In contrast, reduced ADCC activity was observed for a Dab-Fc molecule with a silenced Fc (Fig. S5).²⁷ Thus, the ADCC activity of Dab-Fc is compared to that of an IgG, demonstrating that the molecular composition of the Dab-Fc format does not affect Fc-mediated effector functions.

Inhibition of HER2 and HER3 mediated signaling, proliferation and migration by Dab-Fc-2x3

Homo- and heterodimerization of the HER-family members upon ligand binding leads to activation of the MAPK and the PI3K pathways.⁵ To analyze the effects of the different antibodies on receptor activation and downstream signaling, western blot analyses were performed with HRG-stimulated NCI-N87 cells preincubated with trastuzumab, IgG 3-43, a combination of trastuzumab and IgG 3-43, or Dab-Fc 2 × 3. In the absence of antibodies, stimulation of NCI-N87 cells with HRG resulted in

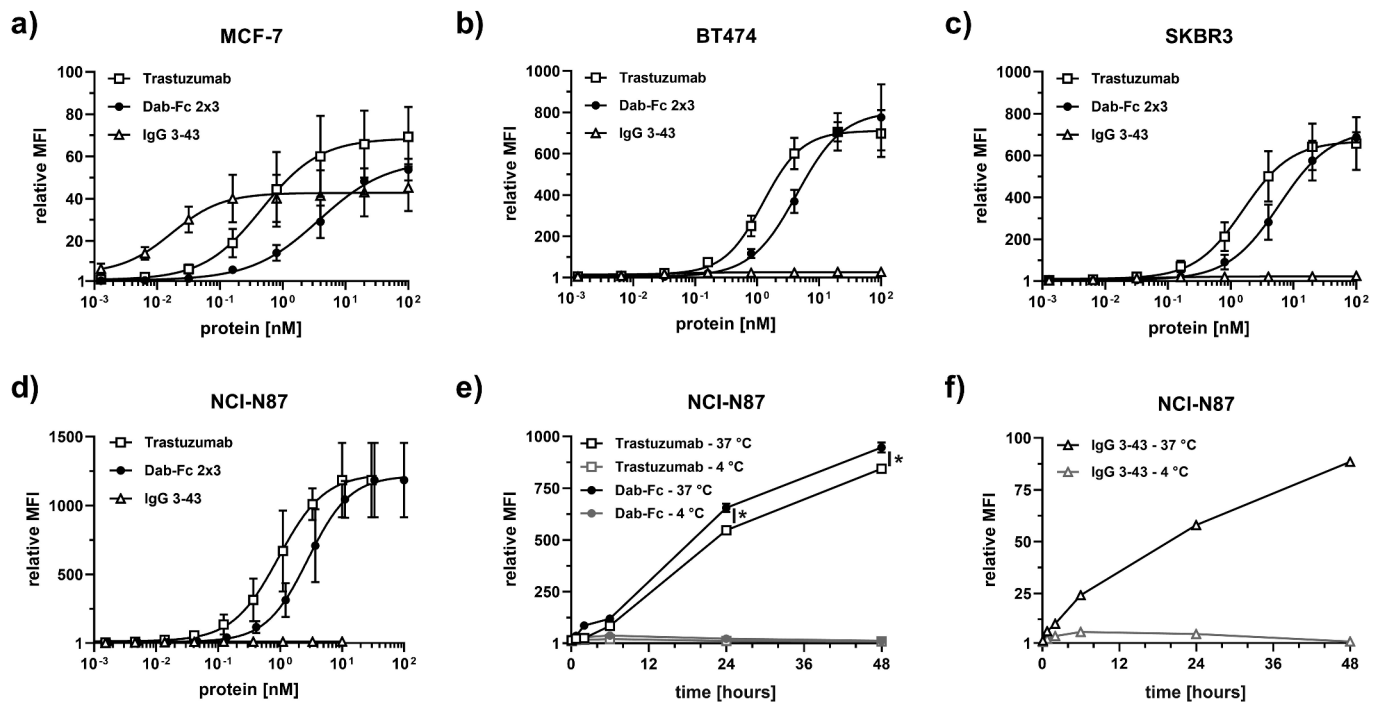


Figure 2. Cell binding and internalization of Dab-Fc 2 × 3 antibody using different tumor cell lines. Binding of the bispecific Dab-Fc 2 × 3 molecule to breast cancer cell lines (MCF-7 (a), BT474 (b), SKBR3 (c)) and the gastric cancer cell-line NCI-N87 (d). Bound antibodies were measured using PE-labeled anti-human Fc secondary antibody. The parental antibodies (trastuzumab and IgG 3–43) were included as a control. Mean ± SD, n = 3. e) and f) internalization of the pHrodo-labeled antibodies was tested using the gastric cancer cell-line NCI-N87 at 37°C and 4°C. Mean ± SD, n = 1, statistics: t-test. *p < .05.

HER3 phosphorylation and the activation of the MAPK and PI3K pathways, as indicated by phosphorylation of ERK and Akt. The bispecific antibody Dab-Fc 2 × 3 strongly inhibited HRG-induced HER3 phosphorylation and activation of the PI3K pathway, while IgG 3–43 alone or in combination with trastuzumab showed only intermediate effects. The constitutive phosphorylation of HER2 in these cells was not affected by any of the antibody treatments (Figure 3).

Next, we analyzed the suppression of basal and HRG-induced survival and proliferation of NCI-N87 cells by Dab-Fc 2 × 3. In the first experiment, cells cultivated in a medium

containing 0.2% serum were treated with either trastuzumab, IgG 3–43, the combination of both antibodies, or the bispecific antibody Dab-Fc 2 × 3 in the absence or presence of HRG. All antibodies reduced HRG-stimulated cell proliferation, with the strongest effects observed for Dab-Fc 2 × 3 (55% compared to 103% for trastuzumab, 83% for IgG 3–43, and 74% for the combination of trastuzumab and IgG 3–43) (Figure 4a).

Furthermore, when seeded at low density, Dab-Fc 2 × 3 strongly reduced the colony formation of NCI-N87 cells by ~70%, while the combination of the parental antibodies showed only a 40% reduction. Different results were observed

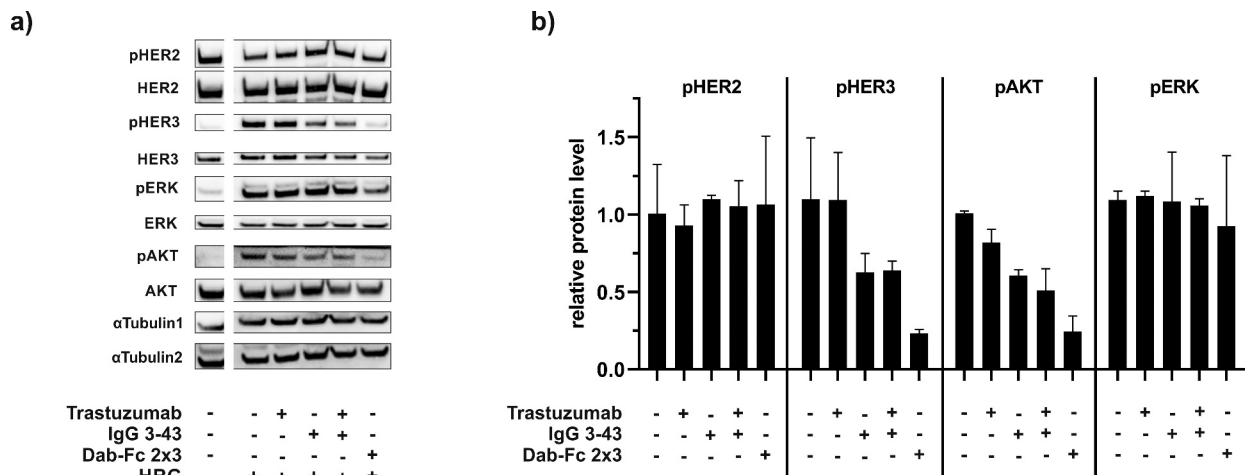


Figure 3. Western blot analysis of receptor phosphorylation and downstream signaling: NCI-N87 cells were starved overnight before treatment with antibodies (trastuzumab, IgG 3–43, combination of trastuzumab and IgG 3–43, or Dab-Fc 2 × 3) for 1 h. After incubation with the antibodies, cells were stimulated with 50 ng/ml HRG for 15 min. a) Subsequently, cell lysates were analyzed by western blot. Signals of unstimulated control cells (left lane) are from the same blot. b) Data shown as mean intensity of signals normalized to α-Tubulin. Mean ± SD, n = 2.

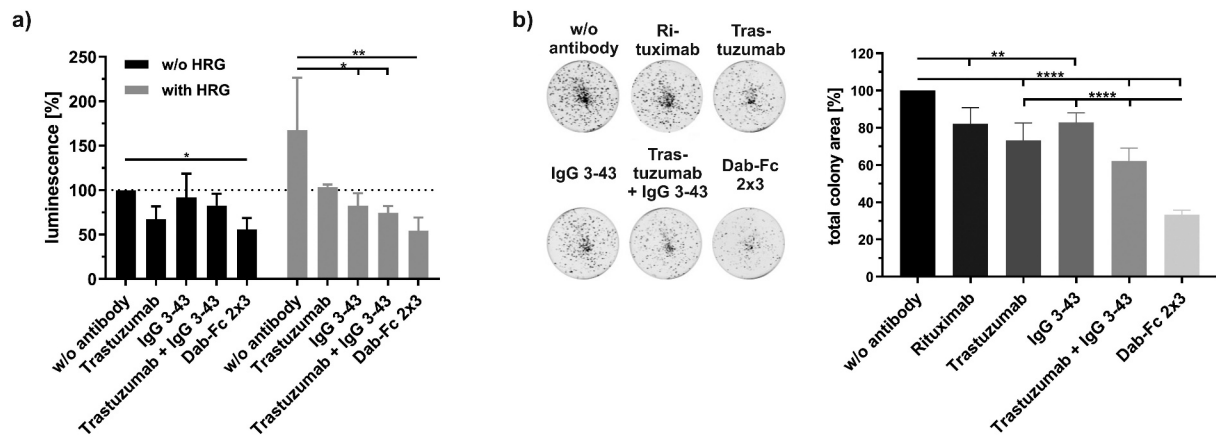


Figure 4. Inhibition of proliferation and colony formation of NCI-N87 cells by Dab-Fc 2 × 3. a) Cells were seeded and on the next day starved with medium containing 0.2% FCS. After cultivating for 24 h, cells were incubated with the different antibodies (100 nM for Dab-Fc; 50 nM for the different antibodies) for 1 h and either left unstimulated (w/o HRG) or stimulated with HRG (25 ng/ml). After 7 days, cells were analyzed using cell titer glo 2.0. Data were normalized to the untreated and unstimulated cells. (n = 3; mean ± SD) statistics: one-way ANOVA. b) Cells were seeded in medium containing 10% FCS. After 24 h of cultivation, cells were treated with 50 nM of the different antibodies or with 100 nM with Dab-Fc molecule in medium containing 2% FCS. After 7 days, cells were retreated with fresh antibodies in 200 µl medium containing 2% FCS. After 12 days of incubation, cells were measured by crystal violet staining. Data were normalized to the untreated cells. Mean ± SD, n = 5, statistics: one-way ANOVA. *p < .05, **p < .01, ***p < .001, ****p < .0001.

for breast cancer cell lines (BT474 and SKBR3 cells) in the colony formation assays (Fig. S6). For BT474 cells, reduction of colony formation by Dab-Fc 2 × 3 was similar to that by trastuzumab (~50%) and stronger than that observed for IgG 3–43 (~30%) or the combination (~40%). For SKBR3 cells, the bispecific antibody Dab-Fc 2 × 3 showed an ~50% reduction of

colony formation, while the parental antibodies reduced colony formation by 30–35%. The strongest effects were detected for the combination of both parental antibodies, with a reduction of 58%.

Since HRG also induces cell migration, we next analyzed the inhibitory effects of Dab-Fc 2 × 3 on cell motility

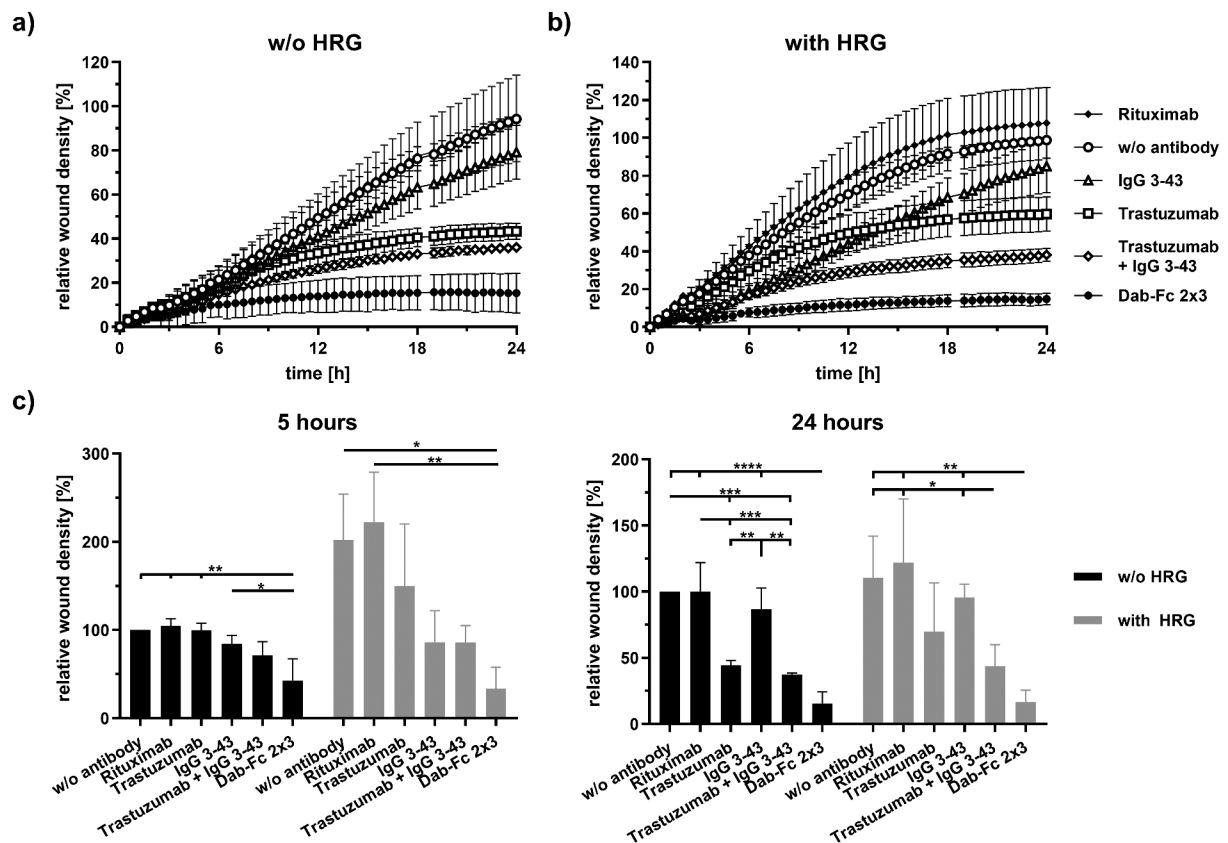


Figure 5. Inhibition of migration of NCI-N87 cells by Dab-Fc 2 × 3. Cells were serum starved (0.2% FCS) for 24 h and a scratch was introduced into confluent cell layer. Cells were then treated with rituximab (negative control), trastuzumab, IgG 3–43, a combination of trastuzumab and IgG 3–43 (each 50 nM), or Dab-Fc (100 nM). Cells were either left unstimulated (a) or were stimulated (b) with 25 ng/ml HRG. Relative wound density was measured for 24 h at 37°C. c) relative wound density after 5 h or 24 h of incubation. Mean ± SD, n = 3, statistics: one-way ANOVA. *p < .05, **p < .01, ***p < .001, ****p < .0001.

in scratch wounding assays. In NCI-N87 cells, basal as well as HRG-induced cell motility was strongly and significantly suppressed by Dab-Fc 2 × 3 when compared to the untreated control cells and as measured by wound closure after 5 hours, and this inhibition was maintained during the 24-h observation period (Figure 5). While Dab-Fc 2 × 3 blocked migration by 85% at this time point, inhibition by the combination of both parental antibodies reached only 37% (-HRG) and 44% (+HRG), respectively. This is most likely due to the potent suppression of the PI3K-Akt pathway, a driver of cell motility, by Dab-Fc 2 × 3 (see Figure 3).²⁸ Inhibition of cell migration was also observed for SKBR3 cells, although the effects were less pronounced but also strongest for Dab-Fc 2 × 3 (Fig. S7). Taken together, the biological activity of the bispecific Dab-Fc 2 × 3 was similar and in many settings even superior to the activity of the parental antibodies.

Pharmacokinetics and anti-tumor activity in an NCI-N87 xenograft model

The pharmacokinetic profile of the bivalent bispecific Dab-Fc 2 × 3 antibody was determined in immunocompetent CD-1 mice receiving a single dose intravenously (i.v.) of Dab-Fc 2 × 3 or the two parental antibodies (trastuzumab, IgG 3–43). Dab-Fc 2 × 3 showed a profile similar to trastuzumab, with terminal half-lives of 117 h (trastuzumab) and 94 hours (Dab-Fc 2 × 3), while the half-life of IgG 3–43 was lower (60 h) (Figure 6a) (Table 3), confirming IgG-like pharmacokinetic properties of the Dab-Fc format.

The anti-tumor activity of the bispecific antibody was analyzed in NCI-N87-bearing SCID-beige mice. Treatment with Dab-Fc 2x3, the parental antibodies alone or in combination, as well as the control (phosphate-buffered saline (PBS)), was initiated when tumor volumes had reached ~100 mm³. Compared to the PBS treatment, IgG 3–43 had no effect on

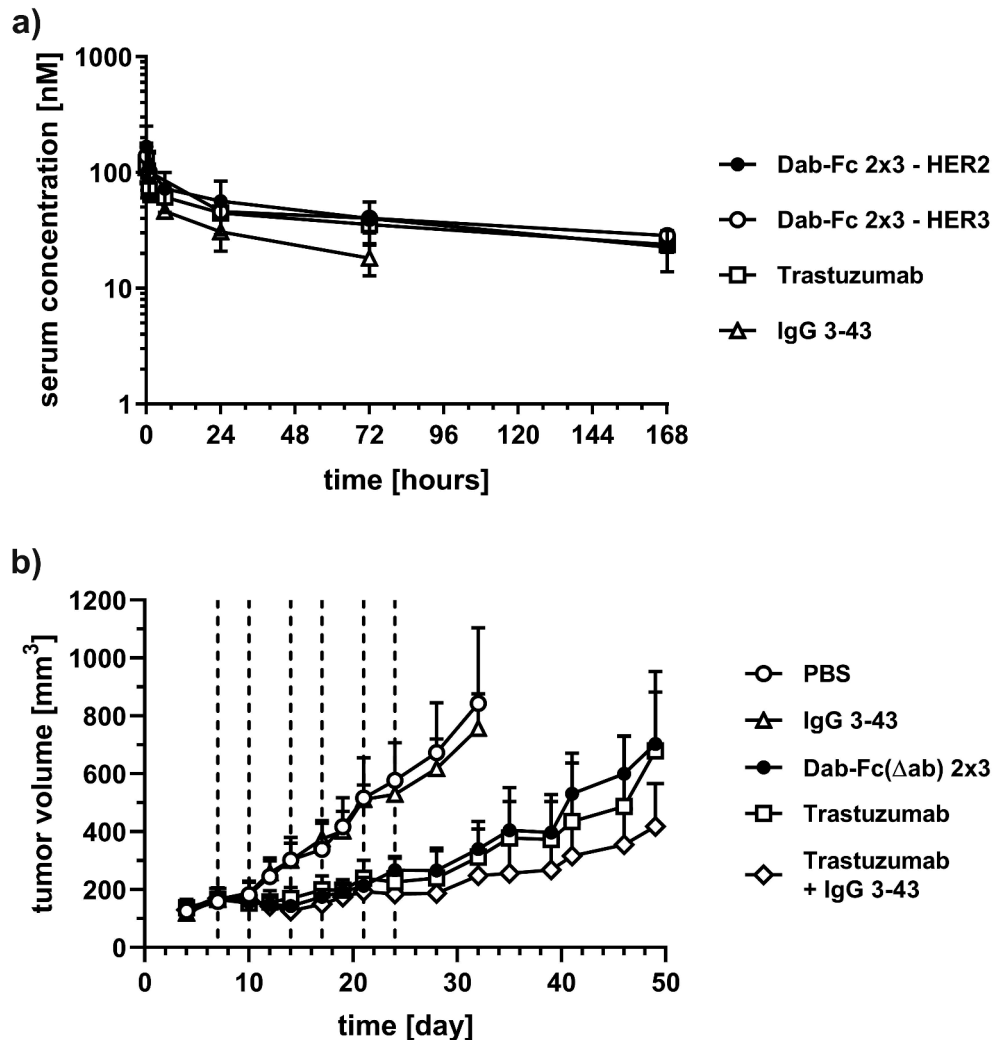


Figure 6. Pharmacokinetics and anti-tumor activity in tumor-bearing mice. a) Pharmacokinetic profile of molecules was analyzed in female CD1 mice ($n = 3$). Mice received a single i.v. injection of 25 μg of the protein. Serum protein concentrations were determined by ELISA using HER2-His and/or HER3-His. Mean \pm 95% CI. b) NCI-N87 cells (5×10^6 cells per dorsal side in combination with 50% matrigel) were inoculated subcutaneously into the left- and right-hand dorsal side of SCID-beige mice. After tumors reached a mean tumor volume of 100 mm^3 mice were treated intravenously with antibodies (trastuzumab, IgG 3–43, combination of both, or Dab-Fc(Δab) 2 × 3) six times (dashed line) in total. Tumor volume was calculated and plotted against the time. Mean \pm 95% CI, $n = 10$ (PBS, trastuzumab, IgG 3–43) or 12 (combination, Dab-Fc(Δab) 2 × 3), statistics: one-way ANOVA. * $p < .05$, ** $p < .01$, *** $p < .001$, **** $p < .0001$.

Table 3. Determination of initial ($t_{1/2\alpha}$) and terminal ($t_{1/2\beta}$) half-lives as well as of drug exposure (area under the curve; AUC) of the parental antibodies and bispecific Dab-Fc 2 × 3 molecule.

	$t_{1/2\alpha}$ [h]		$t_{1/2\beta}$ [h]		AUC [pmol/ml·h]	
	HER2	HER3	HER2	HER3	HER2	HER3
Trastuzumab	0.46 ± 0.36	-	117 ± 22	-	9,812 ± 2,030	-
IgG 3-43	-	1.9 ± 1.8	-	60 ± 32	-	3,898 ± 1,922
Dab-Fc 2x3	0.95 ± 0.47	1.5 ± 0.8	94 ± 4	222 ± 73	9,684 ± 3,779	16,145 ± 4,664

-: not performed; Mean ± SD, n = 3.

tumor size, while Dab-Fc 2 × 3 strongly reduced tumor growth, similar to animals treated with trastuzumab, or the combination of the parental antibodies (Figure 6b). There were no significant differences between the groups treated with trastuzumab, the combinatorial approach, or the bispecific Dab-Fc 2 × 3 molecule during the entire treatment and observation period. The Dab-Fc molecule used for the in vivo study includes a silenced Fc region (Dab-Fc (Δ ab)), and, thus, is not able to exert Fc-mediated effector functions, while the control antibodies possess an unmodified Fc region. A contribution of immune cells, such as macrophages, expressing Fc γ receptors and the activation of the complement system (CMC) to the antitumor effects of the parental antibodies, can therefore not be excluded.

Discussion

Here, we generated a novel bivalent and bispecific antibody Dab-Fc fusion protein with Ig-like properties for dual targeting and inhibition of HER2 and HER3. The key feature of this molecule is a bispecific diabody stabilized by fusion into C_{H1}/C_L domains, thus exhibiting one binding site for each antigen. Fusion of a heterodimerizing Fc region further forces pairing of the cognate V_H and V_L domains and allows purification using affinity resins such as protein G. Furthermore, the Fc region provides IgG-like pharmacokinetic properties due to presumed FcRn-mediated recycling. This was confirmed in the animal study in which the Dab-Fc and trastuzumab showed similar half-lives and drug exposure (AUC). The presence of an Fc region in Dab-Fc 2 × 3 can further contribute to anti-tumor immune responses, such as ADCC.²⁹ In vitro, we could demonstrate in an ADCC assay that the Fc region in the Dab-Fc format fully retained its effector functions.

Dab-Fc 2 × 3 is capable of sequentially binding HER2 and HER3 and combines the neutralizing activities of its parental antibodies. Importantly, Dab-Fc 2 × 3 lacks intrinsic agonistic activity. The HER2 binding site is derived from trastuzumab, which binds to domain IV of HER2 and interferes with receptor dimerization.³⁰ The HER3 binding site is from antibody 3-43, which is capable of inhibiting ligand-dependent and ligand-independent receptor activation.¹⁵ Thus, Dab-Fc 2 × 3 should efficiently inhibit the formation of signaling-competent receptor complexes (either HER2 homodimers or HER2/HER3 heterodimers). This was confirmed in various in vitro assays, in which Dab-Fc 2 × 3 inhibited HER3 receptor phosphorylation and downstream signaling, as well as HRG-induced cell proliferation and migration.

Alternative bispecific molecules targeting HER2 and HER3 were recently described, including a bispecific bivalent IgG

molecule (MCLA-128), a bispecific bivalent scFv-HSA-scFv fusion protein (MM-111), and a tetravalent bispecific IgG-scFv fusion protein, TAB6.²⁰⁻²² Our Dab-Fc 2 × 3 differs from these molecules not only regarding molecular architecture, e.g., geometry, flexibility and distance/orientation of the antigen-binding sites, but also with respect to the parental antibodies, e.g., differing in epitope location. The bivalent bispecific IgG molecule directed against HER2 and HER3 (zenocutuzumab; MCLA-128) is currently under clinical investigation in patients with solid tumors to overcome HER3-mediated resistance to HER2-targeting therapies.^{22,31} The common light-chain antibody uses a “dock & block” mechanism by guiding the HER3-neutralizing activity through binding to HER2. Thus, MCLA-128 binds to domain I of HER2, which is used to guide the HER3 binding arm to HER2-expressing tumor cells, and has itself no inhibitory activity.²² In the scFv-HSA-scFv fusion protein MM-111, the anti-HER2 scFv C6.5 was used, which binds to domain II of HER2 and competes with pertuzumab for binding, thus inhibiting receptor dimerization, while the HER3 binding site is derived from scFv H3, which interferes with HRG-binding to HER3.^{21,32} TAB6 utilizes the trastuzumab IgG fused C-terminally with an scFv derived from the HER3 antibody seribantumab, which binds to domain I of HER3 and inhibits ligand-mediated receptor activation.²⁰ Of note, an increase in proliferation was described for cells incubated with TAB6 but not for the combination of the bivalent parental antibodies. This was explained by a proximity model in which close contacts between HER2 and HER3 are mediated by the tetravalent bispecific antibody leading to receptor activation.²⁰ This is in line with our initial studies, revealing the agonistic activity of a tetravalent bispecific scDb-Fc fusion protein. Altogether, these findings support the application of bivalent and bispecific antibodies for dual targeting of HER2 and HER3.

Dab-Fc retained the internalization capacity of its parental antibodies as shown here with fluorescently labeled antibodies. This might also lead to the uptake and degradation of bound receptors, as shown for HER3 and the parental anti-HER3 antibody IgG 3-43.¹⁵ Western blot studies indicated that Dab-Fc 2 × 3 also induces the internalization of HER3 and its reduction to ~50% after 6 h of incubation (Fig. S4), whereas HER2 levels remained relatively constant, possibly due to the high expression of HER2 in the cell lines investigated. Results from other studies indicate that the internalization of HER2 and bound antibodies depends on receptor expression levels, being more efficient in cells with low expression (<10⁵ receptors/cell) compared to cells with high expression levels (>10⁶ receptors/cell), while recycling of HER2 and bound antibodies back to the plasma membrane is proportional to the HER2

levels.³³ The internalization capacity of trastuzumab was used to develop several antibody-drug conjugates (ADCs), such as ado-trastuzumab emtansine (Kadcyla[®]), approved for treatment of early stage and metastatic HER2-positive breast cancer.³⁴ Recently, it was shown that an anti-HER3 ADC (EV20/MMAF), generated by coupling monomethyl auristatin F (MMAF) through a non-cleavable linker to the anti-HER3 antibody EV20, was highly potent in different HER2-positive tumor models including tumor cells resistant to trastuzumab treatment.³⁵ Bispecific antibodies targeting HER2 and HER3 might further improve the efficacy of ADCs in different tumor settings. Bispecific ADCs are already under development, for instance, targeting HER2 and CD63 to increase the lysosomal delivery mediated by binding to the shuttle protein CD63.³⁶ In another study, a bispecific antibody directed against HER2 and the prolactin receptor (PRLR) demonstrated enhanced HER2 degradation and was more efficient in tumor cell killing than a HER2 ADC.³⁷ Of note, in this study, it was shown that rather low levels of PRLR (~30,000 receptors/cell) were sufficient to mediate effective cell killing.

Importantly, in the gastric cancer cell-line NCI-N87, Dab-Fc 2 × 3 completely blocked HRG-induced cell migration, in agreement with its potent suppression of the PI3K/Akt pathway as a known driver of cell motility.^{38–40} Dab-Fc 2 × 3 might, therefore, particularly interfere with invasiveness and metastasis formation of tumors with HRG-mediated resistance to HER2-targeting therapies, stemming from paracrine secretion of HRG by the stromal cells present in the tumor microenvironment.^{8,41} Although our initial animal experiments using the trastuzumab-sensitive NCI-N87 cell line did not reveal superior effects of the bispecific antibody compared to trastuzumab alone or the combination of the parental antibodies, the situation might be different in trastuzumab-resistant tumors, as shown recently for a resistant NCI-N87 xenograft tumor model treated with a pan-specific HER antibody cocktail.⁴² Thus, further studies are warranted to exploit the full potential of the dual HER2-HER3 targeting antibody Dab-Fc 2 × 3.⁴³

In summary, we successfully applied our versatile Db-Ig platform technology to generate a bivalent bispecific antibody molecule for dual targeting of HER2 and HER3. Dab-Fc 2 × 3 retained its antigen-binding and neutralizing activities and exhibited IgG-like pharmacokinetics, making it a suitable candidate for further therapeutic developments.

Materials and Methods

Materials

For flow cytometry, phycoerythrin (PE)-conjugated anti-human Fc antibody was purchased from Dianova (goat IgG anti-human IgG (Fc)-RPE, 109–115-098; Hamburg, Germany), FITC-conjugated anti-mouse immunoglobulins antibody from Agilent (polyclonal goat anti-mouse Immunoglobulins/FITC, Goat F(ab')₂, F047902–2, Agilent, Waldbronn, Germany), and anti-human HER2 antibody (24D2), anti-human HER3 (1B4C3), anti-human CD3-PE (OKT3), anti-human CD56-APC (5.1H19), and matching isotype controls (MOPC-21; PPV-04) were

purchased from Biologend (purified anti-human CD340 (erbB2/HER-2) antibody, #324402; purified anti-human erbB3/HER-3 Antibody, #324702, Purified anti-human CD3 antibody, #317308; purified anti-human CD56, #981204; Biologend, Fell, Germany). Antibodies for immunoblotting were purchased from Cell Signaling (phospho-HER2/ErbB2) (Tyr1221/1222) (6B12) rabbit mAb #2243; phospho-HER3/ErbB3 (Tyr1289) (21D3) rabbit mAb #4791; Akt (pan) (40D4) mouse mAb #2920; p44/42 MAPK (Erk1/2) (3A7) mouse mAb #9107; phospho-p44/42 MAPK (Erk1/2) (Thr202/Tyr204) antibody #9101; anti-rabbit IgG, horseradish peroxidase (HRP)-linked antibody #7074 (Cell Signaling Technology Europe B.V; Frankfurt am Main, Germany), from Thermo Fisher Scientific (HER-2/c-erbB-2/neu Ab-17, mouse monoclonal antibody #MS-730-P-A; ErbB3, clone: 2F12, Invitrogen[™] mouse mAb #MA5–12675, Schwerte, Germany), from Sigma-Aldrich (α-tubulin mouse mAb #T6793, Taufkirchen, Germany) and Dianova (goat IgG anti-mouse IgG (H + L)-HRP, MinX Hu,Bo,Ho #115-035–062, Hamburg, Germany).

Antibody production and purification

Genes encoding the different polypeptide chains were cloned into a modified pSecTagA vector and were transiently transfected into HEK293–6E suspension cells using polyethylenimine (PEI; linear, 25 kDa, Sigma-Aldrich) for transfection. HEK293–6E cells were provided by National Research Council of Canada (Ottawa, Canada) and cultivated in F17 Freestyle expression medium (ThermoFisher) supplemented with 0.1% (v/v) Kolliphor P-118 (Sigma), 4 mM GlutaMAX (ThermoFisher), and 25 µg/ml G418. By adding TN1 (20% tryptone N1 (Organotechnie S.A.S., France) in F17 medium) to the culture 24 hours post transfection, protein production was initiated and cells were cultivated for additional 4 days at 37°C. Proteins were purified from the supernatant using protein G (ProteinMods, USA) affinity chromatography. Preparations were dialyzed against PBS or Histidine-PBS (10 mM histidine) at 4°C.

Antibody characterization

Antibodies were analyzed by SDS-PAGE (4 µg) and stained with Coomassie-Brilliant Blue G-250. Purity and integrity of molecules (9–30 µg in 30 µl) was analyzed via SEC using a Waters 2695 HPLC in combination with a TSKgel SuperSW mAb HR column (822854, Sigma Aldrich) at a flow rate of 0.5 ml/min using 0.1 M Na₂HPO₄/NaH₂PO₄, 0.1 M Na₂SO₄, pH 6.7 as mobile phase. Standard proteins: thyroglobulin (669 kDa, R_S 8.5 nm), β-amylase (200 kDa, R_S 5.4 nm), bovine serum albumin (67 kDa, R_S 3.55 nm), carbonic anhydrase (29 kDa, R_S 2.35 nm). Stokes radii of antibodies were interpolated from standard proteins. The determination of the aggregation point of the antibody was performed using dynamic light scattering (ZetaSizer Nano ZS, Malvern). Approximately 100 µg of purified protein was diluted to a total volume of 1 ml and

analyzed. The aggregation point was defined as the temperature at which the light scattering increased.

Enzyme-linked immunosorbent assay

The 96-well plates were coated with the extracellular domain (ECD) of HER2-Fc or HER2-His (ECD of HER2: aa 23–652 with C-terminal Fc part or His-tag), or HER3-His (ECD of HER3: aa 20–643 with C-terminal His-tag) (200 ng/well in PBS) overnight at 4°C and residual-binding sites were blocked with 2% (w/v) skim milk powder in PBS (MPBS, 200 µl/well). The antibodies were diluted in MPBS and titrated 1 to 3 in duplicates starting from 100 nM (Dab-Fc) or 30 nM (trastuzumab and IgG 3–43) and incubated for 1 h at room temperature (RT). Bound antibodies were detected with HRP-conjugated antibodies specific for human Fc in case of the antibodies, or specific for His-tag in case of bound HER3-His (excess of 10-fold compared to the antibody in each well). Detection antibodies were incubated for one additional hour at RT. 3,3',5,5'-tetramethylbenzidine (1 mg/ml; 0.006% (v/v) H₂O₂) in a 100-mM Na-acetate buffer, pH 6) was used as a substrate, reaction was terminated using 50 µl 1 M H₂SO₄ and absorption was measured at a wavelength of 450 nm. In general, the plates were washed three times with PBST (PBS + 0.005% (v/v) Tween20) and twice with PBS in between each incubation step and in advance of the detection.

Flow cytometry analysis

The breast cancer cell lines MCF-7, BT-474, and SKBR3, or the gastric cancer cell-line NCI-N87 cells (1x10⁵ per well) were incubated with a serial dilution starting from 100 nM (Dab-Fc), 3 nM (trastuzumab), and 0.3 nM (IgG 3–43) for 1 h at 4°C diluted in PBA (PBS containing 2% (v/v) fetal calf serum (FCS) and 4% (v/v) sodium azide). After washing cells twice, bound antibodies were detected using a PE-labeled anti-human Fc antibody (Jackson ImmunoResearch 109–115-098). Flow cytometry was performed using MACSQuant Analyzer 10 or MACSQuant VYB (both Miltenyi Biotec). Relative median fluorescence intensities (MFI) were calculated as follows: $\text{rel. MFI} = ((\text{MFI}_{\text{sample}} - (\text{MFI}_{\text{detection}} - \text{MFI}_{\text{cells}})) / \text{MFI}_{\text{cells}})$.

Internalization

For the internalization assays, the antibodies (Dab-Fc 2 x 3, trastuzumab, and IgG 3–43) were conjugated with pHrodo label using an NHS labeling moiety (ThermoFisher, P36600). For labeling, antibodies were dialyzed against the buffer and modified with the pHrodo. Proteins were washed afterward with a PD-10 column (GE Healthcare) and binding was analyzed with ELISA. For internalization, the gastric cancer cell-line NCI-N87 (1x10⁵ cells per well) was incubated with the different pHrodo-labeled antibodies (100 nM) either at 37°C or at 4°C. After cultivating of 5 min, 45 min, 2 h, 6 h, 24 h, or 48 h, cells were detached and analyzed by flow cytometry measuring the increase in signal in the PE channel.

Antibody-dependent cellular cytotoxicity assay

ADCC assay was performed using tumor cell lines (NCI-N87) and our bispecific antibody Dab-Fc 2 x 3 either in the absence or in the presence of human PBMCs. For this purpose, 2 x 10⁴ NCI-N87 cells were seeded in an F-bottom 96-well plate in 100 µL RPMI with 10% (v/v) FCS and grown overnight. In addition, PBMCs were thawed and cultivated in a cell culture dish (10 cm) in 10 mL RPMI with 10% (v/v) FCS overnight. On the next day, PBMCs were carefully removed and samples of 100 µL of the suspension were stained with anti-huCD3-PE, anti-huCD56-APC or the isotype controls anti-mouseIgG1-APC and anti-mouseIgG2-PE (all antibodies diluted 1:100 in PBA). After three washing steps with PBA, cells were detected using the MACSQuant[®] Analyzer 10. By analyzing the data in FlowJo Version 10 the proportion of NK cells could be determined (~2–4% of total PBMCs). After pre-incubating the NCI-N87 cells with Dab-Fc 2 x 3, trastuzumab (positive control), and Dab-Fc(Δab) 2 x 3, comprising a silence Fc region (FcΔab: γ chain 1 with mutated residues: E233P, L234V, L235A, ΔG236, A327G, A330S, P331S),²⁷ diluted in RPMI with 10% FCS for 15 minutes, PBMCs were added on top to reach a concentration of 2 x 10⁴ NK cells per well (equals target-to-effector ratio 1:1). Incubation of target cells with antibody in the absence of human PBMCs served as a control. After incubating the plates for 24 h at 37°C, viability of tumor cells was determined by the addition of 50 µL/well crystal violet solution to the remaining target cells. After incubation for 30 min, the plates were washed thoroughly with ddH₂O and dried. The remaining crystal violet was dissolved in 50 µL methanol for 20 min and signals were detected at 550 nm using the Tecan Spark[®] reader. For representation of data as specific lysis, all values were normalized to the control wells containing tumor cells and PBMCs.

Inhibition assay

For downstream signaling analysis, NCI-N87 cells (3.5x10⁵) were seeded into 6-well plates (2 ml, RPMI+10% (v/v) FBS) and incubated for 24 h at 37°C. Next, the medium was exchanged to a starvation medium containing only 0.2% (v/v) FBS. After 24 h, medium was discarded and treatments (trastuzumab, IgG 3–43, combination of trastuzumab and IgG 3–43, or Dab-Fc 2 x 3; 50 nM each) dissolved in 1 ml of starvation medium were added and incubated for 1 h at 37°C. Then, HRG (50 ng) was added to stimulate downstream signaling. After 15 min of incubation, cells were lysed using RIPA lysis buffer (150 mM NaCl), 1% (v/v) Nonidet P-40, 0.5% (w/v) Sodium deoxycholate, 0.1% (w/v) SDS, 25 mM Tris pH 7.4, cOmplete protease inhibitors (Merck, 4693116001). Equal protein amounts of lysates were loaded on NuPage Novex 4–12% Bis-Tris gels (Thermo Fisher Scientific, NP0336). For blotting, the iBlot[™] system was used (Thermo Fisher Scientific, IB301002). Membranes were blocked for 1 h at RT with Roche blocking reagent (Merck, 11096176001), 0.5% (v/v) in PBS containing 0.05% (v/v) Tween-20 (PBST). Membranes were incubated with primary or secondary antibodies diluted in blocking solution at 4°C overnight or 1 h at RT. Between incubation with primary and secondary antibodies, as well as before detection, membranes were washed three times for 5 minutes with PBST. For detection, membranes were incubated with

SuperSignal™ chemiluminescent substrates (Thermo Fisher Scientific, 34075, 34578), followed by imaging using a FUSION SOLO (Vilber Lourmat) device. Signals were quantified using imageJ. For relative protein level, signals were normalized to α -Tubulin signals.

Proliferation assay

NCI-N87 tumor cells (2×10^3 per well) were seeded in 96-well plates and cultivated at 37°C in rich-medium (10% (v/v) FBS) for 24 h and subsequent medium exchange to starvation medium (0.2% (v/v) FBS and 1x penicillin/streptomycin). After 24 hours of starvation, cells were treated with different antibodies (single: 50 nM; combination: 50 nM each; Dab-Fc: 100 nM) for 60 minutes at 37°C. Cells were kept unstimulated or were stimulated with HRG (30 ng/ml; PeproTech; 100–03; Rocky Hill, NJ, USA) and cultivated for 5 days at 37°C. Cell viability was measured using CellTiter-Glo 2.0 Assay (Promega). Luminescence of untreated and unstimulated cells was set as 100%.

Colony formation assay

NCI-N87, BT474, (2×10^3 cells per well) or SKBR3 (3×10^3 cells per well) cells were grown in 12-well plates and cultivated at 37°C in rich-medium (10% (v/v) FBS) for 24 h. Cells were treated with 50 nM rituximab (control), trastuzumab, IgG 3–43, the combination of both trastuzumab and IgG 3–43, or with 100 nM of Dab-Fc 2 \times 3 in a medium with only 2% (v/v) of FBS and 1x penicillin/streptomycin. After incubating cells for 7 days at 37°C, cells were retreated again with the same antibodies for 5 additional days. Then, cells were fixed and analyzed using crystal violet staining.

Migration assay

NCI-N87 (1.3×10^5 cells per well) and SKBR3 (3.5×10^4 cells per well) were seeded in an IncuCyte® ImageLock 96-well plate (Essen BioScience) in a rich medium (containing 10% (v/v) FBS) for 24 hours and subsequent medium exchange to starvation medium (0.2% (v/v) FBS). Scratches were introduced into each well by the WoundMaker® (Essen BioScience). After washing the cells twice with a starvation medium, cells were treated with 50 nM rituximab (control), trastuzumab, IgG 3–43, the combination of both parental antibodies, or with 100 nM of Dab-Fc 2 \times 3 molecule. Cells were either kept unstimulated or were stimulated with HRG (30 ng/ml; PeproTech; 100–03; Rocky Hill, NJ, USA). For a total time of 24 hours, the IncuCyte S3 took images of every well every 30 minutes. Data were analyzed using the Scratch Cell Migration Software Module (Essen BioScience).

Animal experiments

All animal studies were approved by the University of Stuttgart and governmental authorities. For the determination of the pharmacokinetic profile of the different antibodies, the proteins were applied i.v. and blood samples were taken after 3 min, 1 h, 6 h, 24 h, 72 h, and 168 h. After incubation on ice for 20 min, samples were centrifuged (16,000 \times g, 4°C, 20 minutes) and

stored at –20°C until analysis. Serum concentrations of antibodies were determined by ELISA using either HER2-His or HER3-His as immobilized antigen. Bound antibodies were detected with HRP-labeled anti-human Fc secondary antibody. The pharmacokinetics data were calculated with PKSolver.

Anti-tumor activity was studied in tumor-bearing SCID-beige mice. The gastric cancer cell-line NCI-N87 (5×10^6 in 50 μ l) was mixed with 50% (v/v) Matrigel and injected subcutaneously into the left and right dorsal sites of mice. Treatment with the different antibodies was started when the tumor reached a volume of ~ 100 mm³. Mice received i.v. injections of either PBS, IgG 3–43, trastuzumab, the combination of trastuzumab and IgG 3–43, or the bispecific Dab-Fc molecule twice a week for 3 weeks. The initial dose was 150 μ g of IgG 3–43, 150 μ g of trastuzumab (also for the combinatorial approach), and 250 μ g of Dab-Fc (day 7) followed by maintenance doses of 135 μ g of IgG 3–43, 120 μ g of trastuzumab (also for the combination), and 200 μ g of Dab-Fc for the last five injections (day 10, 14, 17, 21, and 24). Tumor volume was measured and calculated as described previously.¹⁵

Statistics

All data are represented as mean \pm SD or \pm 95% CI. Significances were calculated using GraphPad Prism 7.0 and results were compared by one-way ANOVA followed by Tukey's multiple comparison test (posttest) or t-test. $p < .05$ (*), $p < .01$ (**), $p < .001$ (***), $p < .0001$ (****), n.s. (not significant), n.d. (not determined).

Abbreviations:

Antibody drug conjugate (ADC), antibody-dependent cellular cytotoxicity (ADCC), antibody-dependent cellular phagocytosis (ADCP), area under the curve (AUC), constant domain of heavy chain (C_H), constant domain of light chain (C_L), complement-mediated cytotoxicity (CMC), diabody-Fab molecule (Dab), diabody (Db), diabody-immunoglobulin (Db-Ig), extracellular domain (ECD), epidermal growth factor receptor (EGFR), fragment crystalline (Fc), neonatal Fc receptor (FcRn), heregulin (HRG), human serum albumin (HSA), immunoglobulin (Ig), peripheral blood mononuclear cell (PBMC), pharmacokinetic (PK), single-chain diabody (scDb), single-chain Fragment variable (scFv), severe combined immunodeficiency (SCID), triple-negative breast cancer (TNBC), variable domain of heavy chain (V_H), variable domain of light chain (V_L)

Acknowledgments

We would like to thank Nadine Heidel, Doris Göttisch, and Sabine Münkler for excellent technical assistance, as well as Beatrice Reiser and Alexandra Kraske for maintenance of the animal facility. We thank Florian Kast (University of Zurich) for advice regarding the NCI-N87 tumor model. This project was supported by a research grant from SunRock Biopharma S.L. (Spain).











Disclosure of potential conflicts of interest

R.E.K., M.A.O., and O.S. are named inventors on patent applications covering the HER3 antibody and multivalent binding proteins.

Funding

This work was supported by the Deutsche Krebshilfe [70112564]; SunRock Biopharma S.L.

ORCID

Alexander Rau  <http://orcid.org/0000-0001-6810-2714>
 Katharina Kocher  <http://orcid.org/0000-0003-2331-3838>
 Mirjam Rommel  <http://orcid.org/0000-0002-3893-2159>
 Lennart Kühl  <http://orcid.org/0000-0002-6887-8923>
 Maximilian Albrecht  <http://orcid.org/0000-0002-1784-2832>
 Hannes Gotthard  <http://orcid.org/0000-0002-7951-9328>
 Nadine Aschmoneit  <http://orcid.org/0000-0002-9385-9740>
 Monilola A. Olayioye  <http://orcid.org/0000-0003-1093-263X>
 Roland E. Kontermann  <http://orcid.org/0000-0001-7139-1350>
 Oliver Seifert  <http://orcid.org/0000-0003-1876-4212>

References

- Patel A, Unni N, Peng Y. The changing paradigm for the treatment of HER2-positive breast cancer. *Cancers (Basel)*. 2020;12. doi:10.3390/cancers12082081. PMID:32731409.
- Oh D-Y, Bang Y-J. HER2-targeted therapies - a role beyond breast cancer. *Nat Rev Clin Oncol*. 2020;17(1):33–48. doi:10.1038/s41571-019-0268-3. PMID:31548601.
- Melo Gagliato DD, Dlf J, Msp M, Gn H. Mechanisms of resistance and sensitivity to anti-HER2 therapies in HER2+ breast cancer. *Oncotarget*. 2016;7(39):64431–46. doi:10.18632/oncotarget.7043. PMID:26824988.
- Yan M, Parker BA, Schwab R, Kurzrock R. HER2 aberrations in cancer: implications for therapy. *Cancer Treat Rev*. 2014;40(6):770–80. doi:10.1016/j.ctrv.2014.02.008. PMID:24656976.
- Roskoski R. The ErbB/HER family of protein-tyrosine kinases and cancer. *Pharmacol Res*. 2014;79:34–74. doi:10.1016/j.phrs.2013.11.002. PMID:24269963.
- Parakh S, Gan HK, Parslow AC, Burvenich IJG, Burgess AW, Scott AM. Evolution of anti-HER2 therapies for cancer treatment. *Cancer Treat Rev*. 2017;59:1–21. doi:10.1016/j.ctrv.2017.06.005. PMID:28715775.
- Vernieri C, Milano M, Brambilla M, Mennitto A, Maggi C, Cona MS, Prisciandaro M, Fabbioni C, Celio L, Mariani G, et al. Resistance mechanisms to anti-HER2 therapies in HER2-positive breast cancer: current knowledge, new research directions and therapeutic perspectives. *Crit Rev Oncol Hematol*. 2019;139:53–66. doi:10.1016/j.critrevonc.2019.05.001. PMID:31112882.
- Zhang Z, Karthaus WR, Lee YS, Gao VR, Wu C, Russo JW, Liu M, Mota JM, Abida W, Linton E, et al. Tumor microenvironment-derived NRG1 promotes antiandrogen resistance in prostate cancer. *Cancer Cell*. 2020;38(2):279–296.e9. doi:10.1016/j.ccell.2020.06.005. PMID:32679108.
- Campbell MR, Amin D, Moasser MM. HER3 comes of age: new insights into its functions and role in signaling, tumor biology, and cancer therapy. *Clin Cancer Res*. 2010;16(5):1373–83. doi:10.1158/1078-0432.CCR-09-1218. PMID:20179223.
- Amin DN, Campbell MR, Moasser MM. The role of HER3, the unpretentious member of the HER family, in cancer biology and cancer therapeutics. *Semin Cell Dev Biol*. 2010;21(9):944–50. doi:10.1016/j.semcdb.2010.08.007. PMID:20816829.
- Bogoevska V, Wolters-Eisfeld G, Hofmann BT, El Gammal AT, Mercanoglu B, Gebauer F, Vashist YK, Bogoevski D, Perez D, Gagliani N, et al. HRG/HER2/HER3 signaling promotes AhR-mediated Memo-1 expression and migration in colorectal cancer. *Oncogene*. 2017;36(17):2394–404. doi:10.1038/onc.2016.390. PMID:27941874.
- Lee-Hoeflich ST, Crocker L, Yao E, Pham T, Munroe X, Hoeflich KP, Sliwkowski MX, Stern HM. A central role for HER3 in HER2-amplified breast cancer: implications for targeted therapy. *Cancer Res*. 2008;68(14):5878–87. doi:10.1158/0008-5472.CAN-08-0380. PMID:18632642.
- Jaiswal BS, Kljavin NM, Stawiski EW, Chan E, Parikh C, Durinck S, Chaudhuri S, Pujara K, Guillory J, Edgar KA, et al. Oncogenic ERBB3 mutations in human cancers. *Cancer Cell*. 2013;23(5):603–17. doi:10.1016/j.ccr.2013.04.012. PMID:23680147.
- Claus J, Patel G, Ng T, Parker PJ. A role for the pseudokinase HER3 in the acquired resistance against EGFR- and HER2-directed targeted therapy. *Biochem Soc Trans*. 2014;42(4):831–36. doi:10.1042/BST20140043. PMID:25109965.
- Schmitt LC, Rau A, Seifert O, Honer J, Hutt M, Schmid S, Zantow J, Hust M, Dübel S, Olayioye MA, et al. Inhibition of HER3 activation and tumor growth with a human antibody binding to a conserved epitope formed by domain III and IV. *MAbs*. 2017;9(5):831–43. doi:10.1080/19420862.2017.1319023. PMID:28421882.
- Rau A, Lieb WS, Seifert O, Honer J, Birnstock D, Richter F, Aschmoneit N, Olayioye MA, Kontermann RE. Inhibition of tumor cell growth and cancer stem cell expansion by a bispecific antibody targeting EGFR and HER3. *Mol Cancer Ther*. 2020;19(7):1474–85. doi:10.1158/1535-7163.MCT-19-1095. PMID:32430487.
- Santis RD. Anti-ErbB2 immunotherapeutics: struggling to make better antibodies for cancer therapy. *MAbs*. 2020;12(1):1725346. doi:10.1080/19420862.2020.1725346. PMID:32054397.
- Wang L, Yuan H, Li Y, Han Y. The role of HER3 in gastric cancer. *Biomed Pharmacother*. 2014;68(6):809–12. doi:10.1016/j.biopha.2014.08.011. PMID:25194439.
- Baselga J, Swain SM. Novel anticancer targets: revisiting ERBB2 and discovering ERBB3. *Nat Rev Cancer*. 2009;9(7):463–75. doi:10.1038/nrc2656. PMID:19536107.
- Kang JC, Poovassery JS, Bansal P, You S, Manjarres IM, Ober RJ, Ward ES. Engineering multivalent antibodies to target heregulin-induced HER3 signaling in breast cancer cells. *MAbs*. 2014;6(2):340–53. doi:10.4161/mabs.27658. PMID:24492289.
- McDonagh CF, Huhlov A, Harms BD, Adams S, Paragas V, Oyama S, Zhang B, Luus L, Overland R, Nguyen S, et al. Antitumor activity of a novel bispecific antibody that targets the ErbB2/ErbB3 oncogenic unit and inhibits heregulin-induced activation of ErbB3. *Mol Cancer Ther*. 2012;11(3):582–93. doi:10.1158/1535-7163.MCT-11-0820. PMID:22248472.
- Geuijen CAW, Nardis CD, Maussang D, Rovers E, Gallenne T, Hendriks LJA, Visser T, Nijhuis R, Logtenberg T, Kruif JD, et al. Unbiased combinatorial screening identifies a bispecific IgG1 that potently inhibits HER3 signaling via HER2-guided ligand blockade. *Cancer Cell*. 2018;33(5):922–936.e10. doi:10.1016/j.ccell.2018.04.003. PMID:29763625.
- Robinson MK, Hodge KM, Horak E, Sundberg AL, Russeva M, Shaller CC, Mehren MV, Shchavezleva I, Simmons HH, Marks JD, et al. Targeting ErbB2 and ErbB3 with a bispecific single-chain Fv enhances targeting selectivity and induces a therapeutic effect in vitro. *Br J Cancer*. 2008;99(9):1415–25. doi:10.1038/sj.bjc.6604700. PMID:18841159.
- Brinkmann U, Kontermann RE. The making of bispecific antibodies. *MAbs*. 2017;9(2):182–212. doi:10.1080/19420862.2016.1268307. PMID:28071970.
- Seifert O, Rau A, Beha N, Richter F, Kontermann RE. Diabody-Ig: a novel platform for the generation of multivalent and multispecific antibody molecules. *MAbs*. 2019;11(5):919–29. doi:10.1080/19420862.2019.1603024. PMID:30951400.
- Stork R, Müller D, Kontermann RE. A novel tri-functional antibody fusion protein with improved pharmacokinetic properties generated by fusing a bispecific single-chain diabody with an albumin-binding domain from streptococcal protein G. *Protein Eng Des Sel*. 2007;20(11):569–76. doi:10.1093/protein/gzm061. PMID:17982179.
- Armour KL, Clark MR, Hadley AG, Williamson LM. Recombinant human IgG molecules lacking Fcγmamma receptor I binding and monocyte triggering activities. *Eur J Immunol*. 1999;29(8):2613–24. doi:10.1002/(SICI)1521-4141(199908)29:08<2613:AID-IMMU2613><2613:AID-IMMU2613>3.0.CO;2-J. PMID:10458776.

28. Xue G, Hemmings BA. PKB/Akt-dependent regulation of cell motility. *J Natl Cancer Inst.* 2013;105(6):393–404. doi:10.1093/jnci/djs648. PMID:23355761.
29. Graziano RF, Engelhardt JJ. Role of FcγRs in antibody-based cancer therapy. *Curr Top Microbiol Immunol.* 2019;423:13–34. doi:10.1007/82_2019_150. PMID:30790079.
30. Vu T, Claret FX. Trastuzumab: updated mechanisms of action and resistance in breast cancer. *Front Oncol.* 2012;2:62. doi:10.3389/fonc.2012.00062. PMID:22720269.
31. Vries Schultink AHMD, Bol K, Doornbos RP, Murat A, Wasserman E, Dorlo TPC, Schellens JHM, Beijnen JH, Huitema ADR. Population pharmacokinetics of MCLA-128, a HER2/HER3 bispecific monoclonal antibody, in patients with solid tumors. *Clin Pharmacokinet.* 2020;59:875–84. doi:10.1007/s40262-020-00858-2. PMID:32006223.
32. Reddy S, Shaller CC, Doss M, Shchavezleva I, Marks JD, Yu JQ, Robinson MK. Evaluation of the anti-HER2 C6.5 diabody as a PET radiotracer to monitor HER2 status and predict response to trastuzumab treatment. *Clin Cancer Res.* 2011;17(6):1509–20. doi:10.1158/1078-0432.CCR-10-1654. PMID:21177408.
33. Leyton JV. Improving receptor-mediated intracellular access and accumulation of antibody therapeutics—the tale of HER2. *Antibodies (Basel).* 2020;9(3). doi:10.3390/antib9030032. PMID:32668710.
34. Lewis Phillips GD, Li G, Dugger DL, Crocker LM, Parsons KL, Mai E, Blättler WA, Lambert JM, Chari RVJ, Lutz RJ, et al. Targeting HER2-positive breast cancer with trastuzumab-DM1, an antibody-cytotoxic drug conjugate. *Cancer Res.* 2008;68(22):9280–90. doi:10.1158/0008-5472.CAN-08-1776. PMID:19010901.
35. Gandullo-Sánchez L, Capone E, Ocaña A, Iacobelli S, Sala G, Pandiella A. HER3 targeting with an antibody-drug conjugate bypasses resistance to anti-HER2 therapies. *EMBO Mol Med.* 2020;12(5):e11498. doi:10.15252/emmm.201911498. PMID:32329582.
36. Goeij BECGD, Vink T, Napel HT, Breij ECW, Satijn D, Wubbolts R, Miao D, Pwhi P. Efficient payload delivery by a bispecific antibody-drug conjugate targeting HER2 and CD63. *Mol Cancer Ther.* 2016;15(11):2688–97. doi:10.1158/1535-7163.MCT-16-0364. PMID:27559142.
37. Andreev J, Thambi N, Perez Bay AE, Delfino F, Martin J, Kelly MP, Kirshner JR, Rafique A, Kunz A, Nittoli T, et al. Bispecific antibodies and Antibody-Drug Conjugates (ADCs) bridging HER2 and prolactin receptor improve efficacy of HER2 ADCs. *Mol Cancer Ther.* 2017;16(4):681–93. doi:10.1158/1535-7163.MCT-16-0658. PMID:28108597.
38. Wu X, Chen Y, Li G, Xia L, Gu R, Wen X, Ming X, Chen H. Her3 is associated with poor survival of gastric adenocarcinoma: her3 promotes proliferation, survival and migration of human gastric cancer mediated by PI3K/AKT signaling pathway. *Med Oncol.* 2014;31(4):903. doi:10.1007/s12032-014-0903-x. PMID:24623015.
39. Balz LM, Bartkowiak K, Andreas A, Pantel K, Niggemann B, Zänker KS, Brandt BH, Dittmar T. The interplay of HER2/HER3/PI3K and EGFR/HER2/PLC-γ1 signalling in breast cancer cell migration and dissemination. *J Pathol.* 2012;227(2):234–44. doi:10.1002/path.3991. PMID:22262199.
40. Xue C, Liang F, Mahmood R, Vuolo M, Wyckoff J, Qian H, Tsai K-L, Kim M, Locker J, Zhang Z-Y, et al. ErbB3-dependent motility and intravasation in breast cancer metastasis. *Cancer Res.* 2006;66(3):1418–26. doi:10.1158/0008-5472.CAN-05-0550. PMID:16452197.
41. Watanabe S, Yonesaka K, Tanizaki J, Nonagase Y, Takegawa N, Haratani K, Kawakami H, Hayashi H, Takeda M, Tsurutani J, et al. Targeting of the HER2/HER3 signaling axis overcomes ligand-mediated resistance to trastuzumab in HER2-positive breast cancer. *Cancer Med.* 2019;8(3):1258–68. doi:10.1002/cam4.1995. PMID:30701699.
42. Sampera A, Sánchez-Martín FJ, Arpi O, Visa L, Iglesias M, Menéndez S, É G, Dalmases A, Clavé S, Gelabert-Baldrich M, et al. HER-family ligands promote acquired resistance to trastuzumab in gastric cancer. *Mol Cancer Ther.* 2019;18(11):2135–45. doi:10.1158/1535-7163.MCT-19-0455. PMID:31484705.
43. Gómez-Cuadrado L, Tracey N, Ma R, Qian B, Brunton VG. Mouse models of metastasis: progress and prospects. *Dis Model Mech.* 2017;10(9):1061–74. doi:10.1242/dmm.030403. PMID:28883015.